Near-infrared dynamics of photoexcitations in a substituted polyacetylene

Satoshi Takeuchi
Department of Physics University of Tokyo, 7-3-1, Hongo, Bunkyo-ku, Tokyo 113, Japan

Toshio Masuda
Department of Polymer Chemistry, University of Kyoto, Yoshida-Honmachi, Sakyo-ku, Kyoto 606, Japan

Takayoshi Kobayashi
Department of Physics, University of Tokyo, 7-3-1, Hongo, Bunkyo-ku, Tokyo 113, Japan
(Received 15 March 1995)

Near-infrared (0.52–1.37 eV) transient spectra of a substituted polyacetylene, poly[[(*o*-trimethylsilyl)phenyl]acetylene], were measured with a time-resolution better than 300 fs. Whole spectra of hot self-trapped excitons and relaxed, overall neutral pairs of oppositely charged, spatially confined soliton-antisoliton were measured deep in the band gap. The confinement parameter $\gamma=0.23\pm0.07$ and on-site Coulomb repulsion $U_0=2.8\pm0.4$ eV were determined from the results.

I. INTRODUCTION

Nonlinear excitations with geometrical relaxation have been the main subjects of research for quasi-one-dimensional conjugated polymers in relation to their large optical nonlinearities and potential use for applications.[1,2]

A number of spectroscopic works[3] on topological soliton excitations in a degenerate system such as *trans*-polyacetylene have been extensively made so far by means of charge-transfer doping and/or photoexcitation, and successfully explained basically within the frame developed by Su, Schrieffer, and Heeger.[4] The formation process of the soliton, however, has not yet been investigated experimentally because of the difficulties in directly probing the associated in-gap states appearing in the near-infrared (NIR) region with a sufficiently high time resolution. Though the near- to midinfrared (2.5–5.0 μm) photoinduced absorption (PA) of a thin film of *trans*-polyacetylene was previously reported by Rothberg *et al.*,[5] it was measured only at several wavelengths, and did not allow one to discuss the time-dependent spectral shape to disclose the formation process of the soliton. In this paper we report the NIR (0.52–1.37 eV) transient *spectra* of a substituted polyacetylene, poly[[(*o*-trimethylsilyl)phenyl]acetylene] (PMSPA).[6] A broad-band difference-frequency generation as well as a NIR portion of a femtosecond continuum is exploited to cover the spectral region. The temporal variation of the spectral shape observed at early delay times allows us to definitely determine the spectra of both hot self-trapped excitons (STE's) just after photoexcitation and spatially confined, intrachain soliton-antisoliton pairs formed following the charge separation.

A *trans*-rich PMSPA film is preferentially polymerized using a WCl_6 catalyst. The chemical structure of the sample is shown in Fig. 4, and it is written as $(—A=B—)_x$, where $A=CH_2$ and $B=CH\text{-}C_6H_4\text{-}Si(CH_3)_3$. In the limit that the chain is infinitely long ($x\rightarrow\infty$), two configurations with opposite bond alternations, $\cdots—A=B—A=B—A=\cdots$ and $\cdots=A—B=A—B=A—\cdots$, are totally equivalent in energy, because their sterical conformations are identical to each other and only the phase of the bond alternation is different between them. The PMSPA, therefore, has a doubly degenerate ground state to support the formation of the topological soliton excitations as in the case of *trans*-polyacetylene $(—CH=CH—)_x$, polyyne $(—C\equiv C—)_x$,[7] and halogen-bridged mixed-valence complexes.[8] However, a finite chain length of the real sample may lift the ground-state degeneracy by a small amount, and this effectively acts as an attractive force between the two photoexcited charges. An introduced sidegroup also causes a local distortion of the chain. It limits the delocalization of the conjugated π electrons along the chain, which is inferred from a systematic blue shift of the $\pi\rightarrow\pi^*$ interband transition energy observed in several substituted polyacetylenes as compared to that of *trans*-polyacetylene. The attractive force as well as the shortening of the conjugation length confines a photoexcited soliton-antisoliton pair within a segment. The confined soliton-antisoliton pair has been confirmed in this study by a doubly peaked spectrum of the associated in-gap states. The degree of confinement of the solitons and electronic correlation of one-dimensional π electrons, the essential factors in understanding the dynamic behavior of excited species, are to be discussed.

EXPERIMENT

The schematic of the experimental apparatus for pump-probe measurements is shown in Fig. 1. Pulses with a 110 fs duration at 0.8 μm are generated from a Kerr-lens mode-locked, modified Ti sapphire oscillator (Spectra Physics, Model 3900 S) pumped by a 7 W, all-line argon-ion laser (Coherent, INNOVA 310). They seed a Ti:sapphire regenerative amplifier with the optimized cavity design[9] after being stretched temporally up

0163-1829/95/52(10)/7166(5)/$06.00

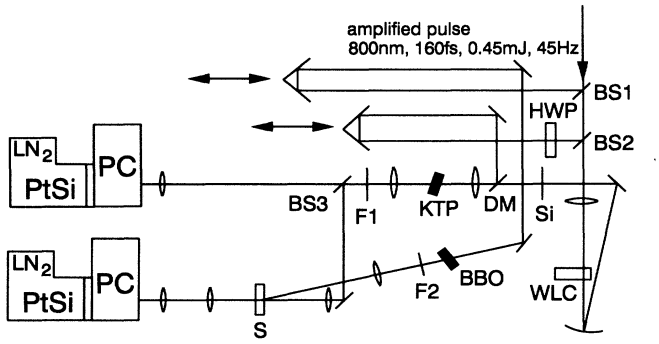

FIG. 1. Schematic drawing of the experimental apparatus for a time-resolved NIR spectroscopy. BS1–3: beam splitters; WLC: glass cell containing CCl_4 for white-light continuum generation; DM: dichroic mirror; Si: silicon-coated plate; F1, F2: filters; S: sample; PC: polychromator: HWP: half-wave plate.

to 120 ps. The amplifier is pumped by an intracavity doubled radiation (5 mJ/pulse at 532 nm) from a continuous-wave pumped, acoustoptically Q-switched Nd:YAG (yttrium aluminum garnet) laser (Clark, ORC-1000) operating at 45 Hz. The pulse energy is amplified to 0.6 mJ during 15–20 round trips. After recompression using a pair of diffraction gratings, we obtain 0.45 mJ pulses with a 160–200 fs duration.

One-third (in energy) of the amplified pulse is split and then frequency doubled ($\lambda=0.4$ μm) in a β-BaB_2O_4 (BBO) crystal (7 mm thick) to excite the sample. The rest is used to generate probe and reference pulses in the NIR region. For measurements in $\lambda=0.90-1.6$ μm a white light continuum is generated in a glass cell (4 mm thick) in which carbon tetrachloride is circulated. After the visible portion of the continuum is filtered, it is divided into probe and reference pulses by a chromium-coated beam splitter. For $\lambda \geq 1.6$ μm a dispersion-free parametric mixing in a $KTiOPO_4$ (KTP) crystal is used to generate a broadband NIR pulse. The parametric process and analysis for the bandwidth were recently investigated in detail elsewhere,[10] and only the outline is described here. The vertically polarized fundamental pulse and horizontally polarized white continuum pulse are collinearly combined by a dichroic mirror and focused into the KTP crystal ($7\times7\times2$ mm^3) cut at $\theta=38.8°$ and $\varphi=90°$ for type-II phase matching ($o=e+o$) in the y-z plane. The parametric mixing enables us to tune the idler (difference-frequency) pulse in the wavelength region of 1.6–2.9 μm by rotating the crystal. The idler bandwidth depends upon the crystal thickness, and it is 700–800 cm^{-1} in the present condition. Only the idler pulse is taken out after collimation by a calcium fluoride (CaF_2) lens, and it is divided into probe and reference pulses using a silicon-coated CaF_2 beam splitter. The probe and reference spectra are measured with two coupled sets of a 120-mm focal-length polychromator and a liquid-nitrogen-cooled platinum silicon (PtSi) multichannel (1024 pixels) infrared detector (EG&G Reticon, RH1024SIU) with a resolution of a ca. 1.9 nm. The pump-probe delay time is scanned by a computer-controlled mechanical stage. The chirping characteristic of the probe pulse is examined by mixing it with the pump pulse in a 0.5-mm-thick BBO crystal prior to measurements. The time resolution of the measurements can be estimated from the half-width at half maximum of the cross-correlation traces, and it ranged within 230–270 fs depending on the probe wavelength. A uniform, thin film of PMSPA was prepared by casting a toluene solution onto a CaF_2 plate and evaporating it slowly under gaseous toluene. The film is quite stable in the air.

RESULTS AND DISCUSSION

Figure 2 shows NIR absorbance change spectra measured at room temperature for several pump-probe delay times together with visible spectra cited from the previous study.[11] At early delay times the NIR spectra show broad PA bands peaking at 1.2–1.4 eV and 0.8–0.9 eV. The PA peak at 1.2–1.4 eV decays faster than the latter, and transient spectra peaking only around 0.8–0.9 eV were observed for delay times longer than 1.0 ps. A minor structure may occur around 0.64 eV, although it is obscured by bumpy structures below 0.8 eV caused partly by a spectral fluctuation of the probe pulse. It is possible that the structure may correspond to a phonon replica of the peak around 0.8–0.9 eV with the energy separation

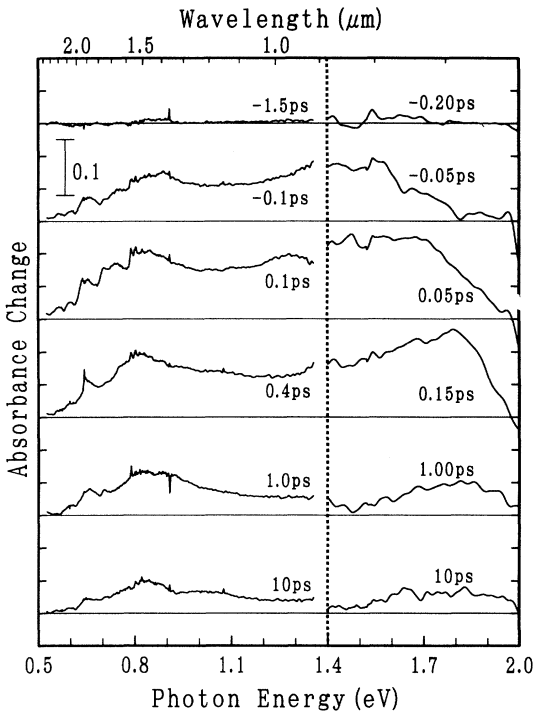

FIG. 2. NIR absorbance change spectra of PMSPA for several delay times measured at room temperature. The polarizations of the pump and probe pulses were parallel to each other, and the excitation density was 2×10^{16} photon/cm^2. Visible spectra above 1.4 eV cited from Ref. 9 are also shown for comparison. Note that both sets of spectra were measured with different time resolutions, i.e., 230–270 fs for the NIR region and 150 fs for the visible region.

nearly equal to the C=C stretching-mode frequency ($\sim 1440\ \mathrm{cm}^{-1}$) or may be due to a polaronic transition as mentioned in Ref. 5. Some spikes on the spectra were due to defects of the detector elements.

The transient spectra in the visible region[11] show that the PA quickly appears around 1.2–1.4 eV with photoexcitation at 2.0 eV. The PA gradually shifts to a peak at 1.8 eV by a delay time of 0.15 ps. Although the excitation photon energies are different in the previous and present studies, both spectra can be compared to reveal the whole electronic spectra from visible to NIR region, because our preliminary measurements with photoexcitation at 2.3 and 4.0 eV also showed similar transient spectra to those with photoexcitation at 2.0 eV, indicating that the photoexcited species are created basically via a π-π^* interband transition rather than an excitonic resonant transition. The instantaneous rise of the PA around 1.2–1.4 eV observed in the NIR spectra is consistent with the behavior at the same energy region in the visible spectra. The entire PA spectrum of the PMSPA thin film, therefore, features a broad peak around 1.2–1.4 eV at early delay times and a doubly peaked (0.8–0.9 and 1.8 eV) structure at delay times longer than 1.0 ps, implying a conversion of photoexcited species occurring within a sub-ps time scale.

We reported before[12] that the temporal behavior of the PA is elegantly accounted for and successfully reproduced by a sum of a power-law decay component and an exponential decay component over the PA region of 1.2–2.0 eV:

$$\Delta A(\nu,t)=A(\nu)\mathrm{erf}[\{\sigma(t-t_d)\}^{-n}] +B(\nu)\exp(-t/\tau)+C(\nu)\ , \quad (1)$$

where erf[ ] is an error function, and the first term is well approximated to the power-law decay, $\sim(t-t_d)^{-n}$, when $t-t_d \geq 1/\sigma$. The first term with $n=0.65$ and $\sigma=4.3$ $(\mathrm{ps})^{-1}$ was evaluated at 1.88 eV, where the PA most likely decays with the power-law behavior. The behavior is characterstic of a geminate recombination process between two photoexcitations which randomly walk on a quasi-one-dimensional chain,[13] and it is distinguished from a monomolecular decay of a single-particle excitation. The power-law component has been interpreted in the previous study to be associated with an intrachain, oppositely charged, overall-neutral, spatially confined soliton-antisoliton pair formed after the photogenerated B_u-symmetric electron-hole pair separates from each other. The power $n=0.5$ is expected for an ideal one-dimensional chain, and the power larger than 0.5 results from the confinement of a soliton-antisoliton pair in a segmented conjugation chain. Even in the finitely long chain $n=0.5$ still holds before the pair feels the segment ends, but thereafter it is theoretically shown that the pair decays with a larger rate.[14] This may lead to the experimentally obtained power larger than 0.5. The geminate recombination results in an A_g-symmetric neutral soliton pair,[15] and it rapidly decays to phonons. The second term with $\tau=135$ fs was evaluated at 1.43 eV. The term is responsible for the instantaneous rise of the PA around 1.2–1.4 eV, and it is due to a hot STE (hot exciton polaron) coupled with lattice vibrations right after photoexcitation,[16] because such a component peaking around 1.2–1.4 eV with an exponential decay is also observed in several other conjugated polymers like polythiophenes and polydiacetylenes.[17,18] This means that the appearance of the exponential component is less affected by the main-chain structure, and that it is not relevant to the ground-state degeneracy in such as the case of soliton formation. The last term, the long-lived component, is possibly due to two-photon excitations and/or other secondary processes between photoexcitations, and is not discussed further here. The introduction of a delay time t_d in the first term in Eq. (1) can reproduce the spectral blueshift observed in the visible region. It was experimentally determined as 98±8 fs and interpreted as a time required for an electron-hole pair to separate spatially to form the confined soliton-antisoliton pair.[12]

The time-independent absorption coefficients, $A(\nu)$ and $B(\nu)$ as a function of probe photon energy ν, show how much each component contributes to the temporal behavior of the PA, and they correspond to decomposed spectra of the confined soliton-antisoliton pair and hot STE, respectively. We have fitted the decay curves below 1.37 eV to Eq. (1) in order to reveal the decomposed spectra. The least-square fitting was made for $A(\nu)$, $B(\nu)$, and $C(\nu)$ with a fixed parameter set: $n=0.65$, $\sigma=4.3$ $(\mathrm{ps})^{-1}$, $t_d=98$ fs, and $\tau=135$ fs. The temporal shape of the cross-correlation trace between the pump and probe pulses was also convoluted with Eq. (1) to take into account the photon-energy dependence of the time resolution. Figure 3 shows the time dependence of the absor-

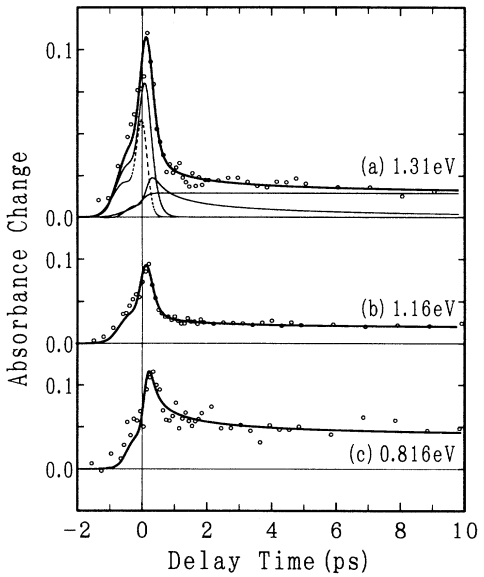

FIG. 3. Time dependence of the absorbance change at probe photon energies of (a) 1.31, (b) 1.16, and (c) 0.816 eV. The experimental data are plotted with circles, and fitted curves to Eq. (1) are shown with bold curves. The three components (thin curves) corresponding to each term of Eq. (1) and the cross-correlation trace (broken curve) are also shown for (a). Note that the vertical scale is expanded in (a).

bance change and fitted curves at three probe photon energies. The three components in Eq. (1) and cross-correlation trace are also included for 1.31 eV. Due to relatively large group-velocity mismatch during the doubling process in the thick BBO crystal, the pump pulse had some structure at the leading edge, making the cross-correlation trace asymmetric. At 1.31 eV the decay is dominated by the exponential component and the absorbance change decreases down to a quarter of the initial value by 1 ps, while the power-law component dominates the slowly decaying behavior at 0.816 eV. The time dependence of the absorbance change is well reproduced by Eq. (1) over the entire PA region, and this confirms the validity to decompose the PA into the spectral superposition of the power-law and exponential components.

Figure 4 shows $A(\nu)$ and $B(\nu)$ plotted against probe photon energy together with the stationary absorption spectrum of PMSPA. The data points above 1.35 eV are cited from our previous study.[12] The fitting errors (i.e., standard deviations obtained in the fitting procedure) for $A(\nu)$ and $B(\nu)$ are smaller than 1.3×10^{-2} and 1.9×10^{-2}, respectively, for the region above 1.35 eV, and those below 1.35 eV are shown in the figure. The decomposed spectrum of the confined soliton-antisoliton pair is doubly peaked at $E_L=0.82$ eV and $E_H=1.8$ eV with a valley around 1.1–1.2 eV, while that of the hot STE has a peak at 1.4 eV with a full width at half maximum of 0.72 eV. These spectral shapes are revealed in the present study.

The doubly peaked spectrum $A(\nu)$ implies that the in-gap states associated with the confined soliton-antisoliton pair is well split into two isolated levels unlike the degenerate case in the independent electron model. The overlap of the soliton wave functions due to their confinement within a segmented conjugation chain of the polymer is the most probable origin for the split. The ground-state degeneracy may be lifted slightly by a finite length of the chain and a limited conjugation. The energetically unfavored configuration appears between the soliton and antisoliton in this case, and the increase of energy proportional to the size of the configuration makes them attract to each other. The π-conjugation length is shortened by torsional defects due to a bulky sidegroup attached to every two carbon sites, also limiting the spatial separation of the soliton and antisoliton. The two peak energies are located assymmetrically with respect to the gap center at $\Delta=E_g/2=1.1$ eV, implying that an electronic correlation plays an important role. Here we assume that the high-energy (HE) and low-energy (LE) *one-electron* in-gap levels are located respectively at $+\omega_0$ and $-\omega_0$ symmetrically around the gap center. Both the HE and LE levels are singly occupied for the B_u-symmetric soliton-antisoliton pair. The lower transition energy, corresponding to the promotion of an electron from the valence band (VB) to the LE level or that from the HE level to the conduction band (CB), is expressed as $E_L=\Delta-\omega_0+U_C$, where U_C is an effective electronic correlation energy. In the same way, the higher transition energy, corresponding to the promotion of an electron from the VB to the HE level or that from the LE level to the CB, is expressed as $E_H=\Delta+\omega_0+U_C$. The transition energies are thus located symmetrically around $\Delta+U_C$, not the gap center (Δ). The stimulated transition between the HE and LE levels is suppressed because of the same occupation numbers for the two levels and the decreased overlap of the wave functions. From their separation, $\omega_0=(E_H-E_L)/2=0.49$ eV and $U_C=(E_H+E_L)/2-\Delta=0.21$ eV are obtained. Though the microscopic, onsite Coulomb repulsion U_0 is to be derived with some care, we roughly estimate it here using the first-order perturbation theory as $U_0\sim3(l/a)U_C$, a being a carbon-carbon distance.[19] The size of a soliton in PMSPA, $l=(4.5\pm0.5)a$,[11] yields $U_0=2.8\pm0.4$ eV. The value is close to the transfer energy ($t_0\sim2.5$ eV) of π electrons, indicating that the system is weakly correlated ($U_0<4t_0$) and still in the Peierls regime.[20]

The in-gap level splitting also becomes an effective probe for the degree of confinement (DOC) of charges. In addition to the extrinsic origin that a segmented conjugation chain confines the photogenerated charge carriers, it is theoretically predicted[21] that the Coulombic attraction between the two oppositely charged solitons forms a bound soliton-antisoliton pair even in the exactly degenerate system without any distortions. The dynamic behavior of photogenerated species is supposed to be closely correlated with the DOC. One of its measure, the confinement parameter, defined as $\gamma=p\sin^{-1}p/(1-p^2)^{1/2}$ with $p\equiv\omega_0/\Delta$, has been referred so far to compare the DOC in a number of polymers. For the case of PMSPA, $\omega_0=0.49$ eV and $\Delta=1.1$ eV yield $\gamma=0.23\pm0.07$. It is an experimental report for a short-lived species. An average distance of $\sim7.5a$ between the two solitons is inferred with this DOC. To elucidate the relation between the formation and/or decay process and the DOC in various systems is the next step to obtain the microscopic picture for the dynamics of solitons.

The spectral peak at 1.4 eV for the hot STE was discussed before, and it corresponds to the promotion of an

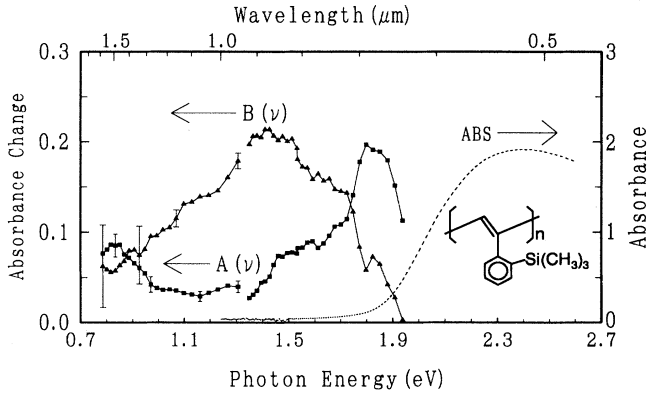

FIG. 4. Fractions of the confined soliton-antisoliton pair (A) and hot STE (B) components plotted against probe photon energy ν. The chemical structure of PMSPA and its stationary absorption spectrum (broken curve) are also shown.

electron from the hot STE state possibly to the CB. The large binding energy of 1.4 eV is theoretically predicted for one-dimensional excitons, and it is attributable to both the bare Coulombic binding energy and lattice stabilization energy.[22] The transient lattice relaxation has been recently studied by molecular dynamics taking both the electron-phonon coupling and electronic correlation into account.[23] It reveals that an exciton couples with the lattice vibrations and exchanges its energy back and forth with the lattice before an irreversible energy transfer taking place at several tens of femtoseconds. In the initial stage of relaxation the binding energy of the exciton was calculated to oscillate at 1.56 ± 0.06 eV with the on-site Coulomb repulsion $U_0=2.4$ eV. The binding energy is consistent with the experimental observation, and the value of U_0 agrees quite well with that estimated from the decomposed spectrum of the confined soliton-antisoliton pair. The broad spectral width of 0.72 eV is supposed to result from nonthermal population distribution in the vibrational manifolds with the exchange of energy as well as a statistical distribution of the conjugation length.

CONCLUSION

A femtosecond pump-probe experiment was performed in the near-infrared (0.52–1.37 eV) region, and the transient spectra of a substituted polyacetylene, poly[[(*o*-trimethylsilyl)phenyl]acetylene], were measured deep in the band gap. Comparing them with the visible data, the photoinduced absorption band features a broad peak around 1.2–1.4 eV at early delay times and a doubly peaked structure at delay times longer than 1 ps. The time-dependent spectral shape has been elegantly reproduced by a spectral superposition of an exponential and a power-law decay components. The exponential component peaking at 1.4 eV corresponds to a hot self-trapped exciton right after photoexcitation, while the power-law component doubly peaked at $E_L=0.82$ eV and $E_H=1.8$ eV is due to an intrachain, oppositely charged, overall-neutral, spatially confined soliton-antisoliton pair.

The in-gap level splitting $2\omega_0=0.98$ eV for the soliton-antisoliton pair and the effective electronic correlation energy $U_c=0.21$ eV have been independently evaluated from the doubly peaked spectrum. The splitting is due to the spatial overlap of the soliton and antisoliton wave functions resulting from their confinement in a segmented conjugation chain. The degree of confinement is characterized by a confinement parameter $\gamma=0.23\pm0.07$.

The peak at 1.4 eV for the hot self-trapped exciton corresponds to a transition to the conduction band edge. The peak energy is fairly consistent with the results of the molecular dynamics including both electron-phonon and electron-electron interactions.

ACKNOWLEDGMENTS

The authors are grateful to Dr. K. Ishida for stimulating discussions. This work was partly supported by the Grant-in-Aid for Specially Promoted Research No. 05102002.

[1] *Relaxation in Polymers,* edited by T. Kobayashi (World Scienctific, Singapore, 1993).
[2] Z. V. Vardeny, Chem. Phys. **177**, 743 (1993).
[3] A. J. Heeger, S. Kivelson, J. R. Schrieffer, and W. P. Su, Rev. Mod. Phys. **60**, 781 (1988), and references therein.
[4] W. P. Su, J. R. Schrieffer, and A. J. Heeger, Phys. Rev. Lett. **42**, 1698 (1979).
[5] L. Rothberg, T. M. Jedju, P. D. Townsend, S. Etemad, and G. L. Baker, Mol. Cryst. Liq. Cryst. **194**, 1 (1991).
[6] T. Masuda, T. Hamano, K. Tsuchihara, and T. Higashimura, Macromolecules **23**, 1374 (1990).
[7] M. J. Rice, S. R. Phillpot, A. R. Bishop, and D. K. Campbell, Phys. Rev. B **34**, 4139 (1986).
[8] Y. Onodera, J. Phys. Soc. Jpn. **56**, 250 (1987).
[9] S. Takeuchi and T. Kobayashi, Opt. Commun. **109**, 518 (1994).
[10] S. Takeuchi and T. Kobayashi, J. Appl. Phys. **75**, 2757 (1994).
[11] S. Takeuchi, M. Yoshizawa, T. Masuda, T. Higashimura, and T. Kobayzashi, IEEE J. Quantum Electron. **QE-28**, 2508 (1992).
[12] S. Takeuchi, T. Masuda, T. Higashimura, and T. Kobayashi, Solid State Commun. **87**, 655 (1993).
[13] C. V. Shank, R. Yen, R. L. Fork, J. Orenstein, and G. L. Baker, Phys. Rev. Lett. **49**, 1660 (1982).
[14] I. V. Zozulenko, Solid State Commun. **76**, 1035 (1990).
[15] T. W. Hagler and A. J. Heeger, Chem. Phys. Lett. **189**, 333 (1992).
[16] M. Nisoli, A. Cybo-Ottone, S. De Silvestri, V. Magni, R. Tubino, S. Luzzati, A. Musco, and D. Comoretto, Solid State Commun. **86**, 583 (1993).
[17] T. Kobayashi, M. Yoshizawa, U. Stamm, M. Taiji, and M. Hasegawa, J. Opt. Soc. Am. B **7**, 1558 (1990).
[18] U. Stamm, M. Taiji, M. Yoshizawa, K. Yoshino, and T. Kobayashi, Mol. Cryst. Liq. Cryst. **182A**, 147 (1990).
[19] D. Baeriswyl, D. K. Campbell, and S. Mazumdar, Phys. Rev. Lett. **56**, 1509 (1986).
[20] G. W. Hayden and E. J. Mele, Phys. Rev. B **34**, 5484 (1986).
[21] M. Grabowski, D. Hone, and J. R. Schrieffer, Phys. Rev. B **31**, 7850 (1985).
[22] S. Abe, J. Yu, and W. P. Su, Phys. Rev. B **45**, 8264 (1992).
[23] K. Ishida, Solid State Commun. **90**, 89 (1994).